# Interphotoreceptor retinoid–binding protein removes all-*trans*-retinol and retinal from rod outer segments, preventing lipofuscin precursor formation

Received for publication, May 9, 2017, and in revised form, September 22, 2017 Published, Papers in Press, September 28, 2017, DOI 10.1074/jbc.M117.795187

**Chunhe Chen[‡], Leopold Adler IV[‡], Patrice Goletz[‡], Federico Gonzalez-Fernandez[§], Debra A. Thompson[¶1], and Yiannis Koutalos[‡2]**

*From the [‡]Departments of Ophthalmology and Neurosciences, Medical University of South Carolina, Charleston, South Carolina 29425, the [§]Departments of Ophthalmology and Pathology, University of Mississippi and G. V. (Sonny) Montgomery Veterans Affairs Medical Centers, Jackson, Mississippi 39216, and the [¶]Departments of Ophthalmology and Visual Sciences, and Biological Chemistry, University of Michigan School of Medicine, Ann Arbor, Michigan 48105*

Edited by F. Peter Guengerich

**Interphotoreceptor retinoid–binding protein (IRBP) is a specialized lipophilic carrier that binds the all-*trans* and 11-*cis* isomers of retinal and retinol, and this facilitates their transport between photoreceptors and cells in the retina. One of these retinoids, all-*trans*-retinal, is released in the rod outer segment by photoactivated rhodopsin after light excitation. Following its release, all-*trans*-retinal is reduced by the retinol dehydrogenase RDH8 to all-*trans*-retinol in an NADPH-dependent reaction. However, all-*trans*-retinal can also react with outer segment components, sometimes forming lipofuscin precursors, which after conversion to lipofuscin accumulate in the lysosomes of the retinal pigment epithelium and display cytotoxic effects. Here, we have imaged the fluorescence of all-*trans*-retinol, all-*trans*-retinal, and lipofuscin precursors in real time in single isolated mouse rod photoreceptors. We found that IRBP removes all-*trans*-retinol from individual rod photoreceptors in a concentration-dependent manner. The rate constant for retinol removal increased linearly with IRBP concentration with a slope of 0.012 $min^{-1}$ $\mu M^{-1}$. IRBP also removed all-*trans*-retinal, but with much less efficacy, indicating that the reduction of retinal to retinol promotes faster clearance of the photoisomerized rhodopsin chromophore. The presence of physiological IRBP concentrations in the extracellular medium resulted in lower levels of all-*trans*-retinal and retinol in rod outer segments following light exposure. It also prevented light-induced lipofuscin precursor formation, but it did not remove precursors that were already present. These findings reveal an important and previously unappreciated role of IRBP in protecting the photoreceptor cells against the cytotoxic effects of accumulated all-*trans*-retinal.**

This work was supported in part by National Institutes of Health Grants R01-EY014850 (to Y. K.) and R01-EY09412 (to F. G.-F.), Merit Review Award I01BX007080 from the Biomedical Laboratory Research and Development Service of the Veterans Affairs Office of Research and Development (to F. G.-F.), and a start-up award from Research Mississippi, Inc. (to F. G.-F.). The authors declare that they have no conflicts of interest with the contents of this article. The content is solely the responsibility of the authors and does not necessarily represent the official views of the National Institutes of Health or the Veterans Affairs.

[1] Recipient of Research to Prevent Blindness Senior Scientific Investigator Award.

[2] To whom correspondence should be addressed: Dept. of Ophthalmology, Medical University of South Carolina, 167 Ashley Ave., Charleston, SC 29425. Tel.: 843-792-9180; Fax: 843-792-1723; E-mail: koutalo@musc.edu.

Detection of light by the rod photoreceptor cells in the vertebrate retina begins in the outer segment, an organelle that is packed with the visual pigment rhodopsin, the primary light detector. The light-detecting chromophore of rhodopsin is 11-*cis*-retinal, which is isomerized by light to all-*trans*; the photoisomerization activates rhodopsin and begins the reactions of visual transduction (1, 2). Photoactivated rhodopsin eventually dissociates to all-*trans*-retinal and the protein component opsin. All-*trans*-retinal is a reactive aldehyde with a range of deleterious effects and is removed through reduction to all-*trans*-retinol.[3] The reduction of all-*trans*-retinal to all-*trans*-retinol occurs primarily in photoreceptor outer segments in a reaction that is catalyzed by retinol dehydrogenase RDH8 (3–5) and requires metabolic input in the form of NADPH (6, 7). The reduction of all-*trans*-retinal that leaks into photoreceptor inner segments is catalyzed by the broad specificity retinol dehydrogenase RDH12 (3, 8). All-*trans*-retinal that escapes reduction to all-*trans*-retinol forms lipofuscin precursors (LFPs),[4] such as bis-retinoids, the condensation products of two retinal molecules (9, 10). Bis-retinoid adducts are a major component of lipofuscin (11), a fluorescent pigment mixture that accumulates in the lysosomes of the retinal pigment epithelium (RPE), and it has been associated with the development of degenerative diseases of the retina, such as age-related macular degeneration and Stargardt disease.

The all-*trans*-retinol generated from the reduction of all-*trans*-retinal is transported out of the rod outer segments and into the adjacent cells of the RPE, where it is recycled to form 11-*cis*-retinal (12–14). 11-*cis*-Retinal is transported from the RPE to the rod outer segments where it combines with opsin to reform rhodopsin. Retinoids have low aqueous solubility (15), and their transport through aqueous space is supported by specialized carriers (16). Such a carrier, the interphotoreceptor retinoid–binding protein (IRBP), is the major soluble protein

[3] When the isomer is not specified, retinal and retinol refer to the all-*trans* isomers.

[4] The abbreviations used are: LFP, lipofuscin precursor; IPM, interphotoreceptor matrix; IRBP, interphotoreceptor retinoid-binding protein; RAL, all-*trans*-retinal; ROL, all-*trans*-retinol; bROS; broken-off rod outer segments; RPE, retinal pigment epithelium. When the isomer is not specified, retinal and retinol refer to the all-*trans* isomers.

present in the interphotoreceptor matrix (IPM), the material between the photoreceptor outer segments and the RPE (17, 18). IRBP binds the 11-*cis* and all-*trans* isomers of both retinal and retinol (19), and it promotes the transfer of all-*trans*-retinol from photoreceptors to RPE (20) and of 11-*cis*-retinal in the opposite direction (21). IRBP's role in this trafficking may not be in its transport role *per se* (22, 23) rather than an ability to protect these retinoids from photodecomposition (24–26). Defects in IRBP cause retinal degenerations in individuals with mutations in the *RBP3* gene (27) and *Rbp3*-null transgenic mice (28). A protective role for IRBP may also be associated with facilitating the clearance of all-*trans*-retinal generated by light in rod outer segments, which would be promoted by the removal of all-*trans*-retinol and perhaps of all-*trans*-retinal itself.

The levels of all-*trans*-retinol, all-*trans*-retinal, and lipofuscin precursors can be measured in single rod photoreceptors by imaging their fluorescence (29). The removal of all-*trans*-retinol by IRBP has been previously characterized with single cell fluorescence imaging in the large photoreceptor cells from amphibian retinas (30). In this study, we have used fluorescence imaging to characterize the effects of IRBP on all-*trans*-retinol, all-*trans*-retinal, and lipofuscin components in the much smaller and fragile mouse rod photoreceptors. We found that IRBP can remove both all-*trans*-retinol and all-*trans*-retinal in a concentration-dependent manner while preventing the formation of lipofuscin precursors that accumulate with aging and disease in the mammalian retina.

## Results

### *Retinal degeneration in Irbp-deficient mice*

Irbp-deficient ($Rbp3^{-/-}$) mice exhibit early-onset retinal degeneration that is evident in photomicrographs of animals as young as 1 month of age (28), and the morphometric measurements of outer nuclear layer thickness show progress to severe disease by 1 year of age (Fig. 1). While affirming the critical role of IRBP in retinal function, the massive photoreceptor cell death occurring in the knock-out-mouse model limits its usefulness for studies of the visual cycle mechanism. Thus, we focused our efforts on single-cell fluorescence imaging of the effects of IRBP on the levels of all-*trans*-retinal, all-*trans*-retinol, and lipofuscin precursors present in isolated rod photoreceptor cells from wild-type and other visual cycle mutant strains.

### *Removal of all-trans-retinol by IRBP*

In dark-adapted mouse rod photoreceptors, there is an increase in outer segment fluorescence excited by UV light (excitation, 360 nm; emission, >420 nm) following rhodopsin bleaching (31). In the case of metabolically intact rods, this fluorescence is due overwhelmingly to the all-*trans*-retinol formed from the reduction of the all-*trans*-retinal released by photoactivated rhodopsin (3, 6). In single isolated rods, and in the absence of extracellular lipophilic carriers, fluorescence reaches a peak ~30 min after bleaching and then declines as retinol slowly leaves the outer segment. Fig. 2*A* shows an experiment with an isolated wild-type mouse rod photoreceptor that was bleached in the absence of lipophilic carriers.

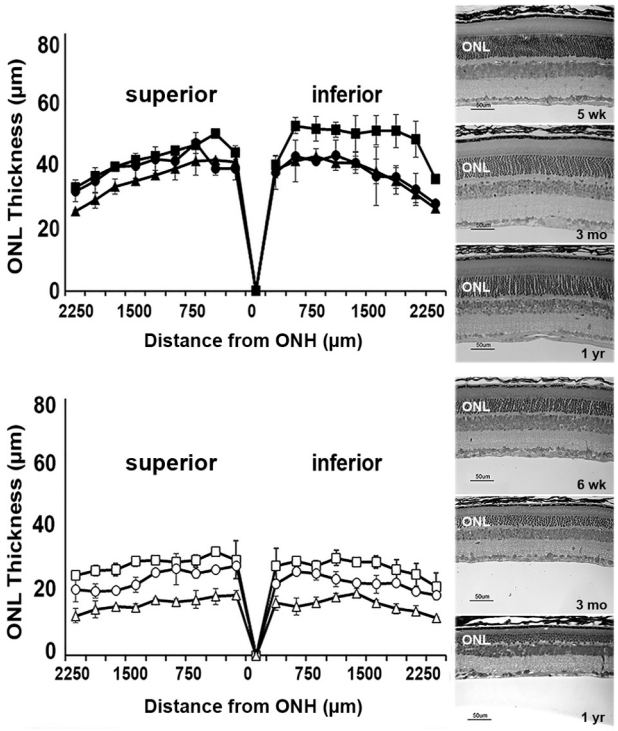


**Figure 1. Irbp-deficient mice exhibit early and progressive photoreceptor cell loss.** Eyes from wild-type (C57BL/6) and Irbp-deficient ($Rbp3^{-/-}$) mice were fixed in 2% paraformaldehyde and 2% glutaraldehyde, embedded in JB-4 plastic, and Lee's stained sections of retina/RPE/choroid (5 $\mu$m) were imaged on a Nikon Eclipse E800 microscope with DMX1200 digital camera. Measurements of outer nuclear layer (*ONL*) thickness obtained using Image ProPlus 5.0 software were plotted *versus* distance from the optic nerve head (*ONH*) ± S.D. and are shown alongside representative micrographs of the superior retina about 500 $\mu$m from the optic nerve. *Top,* C57BL/6 mice: 5 weeks (■, $n = 3$); 3 months (●, $n = 3$); 1 year (▲, $n = 5$). *Bottom,* Irbp-deficient mice: 6 weeks (□, $n = 3$); 3 months (○, $n = 3$); 1 year (△, $n = 4$).

After bleaching, there was a large increase in outer segment fluorescence due to the formation of all-*trans*-retinol; at 30 min after bleaching IRBP was added to the extracellular medium at a final concentration of 2 $\mu$M, and the outer segment fluorescence declined rapidly. This was a single experiment at one IRBP concentration. The experiment was repeated with different cells and with different concentrations of IRBP. The results from these experiments, showing the decline of outer segment fluorescence as a function of IRBP concentration, are plotted in Fig. 2*B*. To facilitate comparisons across cells and IRBP concentrations, the outer segment fluorescence was normalized to its value immediately after the addition of IRBP, and the data were then averaged. It appears that all of the all-*trans*-retinol generated by bleaching can be removed by IRBP, because at higher IRBP concentrations (10 and 20 $\mu$M), the outer segment fluorescence had declined to its pre-bleach value by the end of the experiment. For each IRBP concentration, single exponentials, $e^{-k \cdot t}$, decaying to 0 with unitary amplitude at $t = 0$ min, were fitted through the fluorescence data. The fits provided the first-order rate constants for all-*trans*-retinol removal at each concentration of IRBP.

The rate constant of all-*trans*-retinol removal increased with the IRBP concentration ($p = 0.0001$; linear regression). The

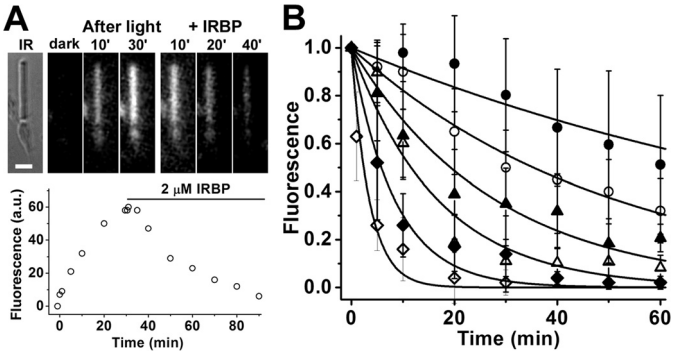


**Figure 2. Measurement of all-*trans*-retinol removal by different concentrations of IRBP in isolated metabolically intact rod photoreceptors from wild-type mice.** *A,* removal of all-*trans*-retinol formed after bleaching by 2 $\mu$M IRBP. *IR,* infrared image of a single rod photoreceptor showing its straight outer segment over the rounded tapered inner segment; *bar,* 5 $\mu$m. Bleaching was carried out between $t = -1$ min and $t = 0$; IRBP was added 30 min after bleaching. Fluorescence images of the cell were acquired with 360 nm excitation and >420 nm emission. *B,* removal of all-*trans*-retinol by different concentrations of IRBP added at $t = 0$, 30 min after the bleaching of rhodopsin. Retinol outer segment fluorescence intensities have been normalized over the value at $t = 0$. The *lines* are simple exponentials, $e^{-k \cdot t}$, decaying to 0 with unitary amplitude at $t = 0$ min; they have been drawn with rate constants $k$ determined from the experimental data points. Without addition of IRBP, retinol fluorescence decreased with a rate constant 0.009 ± 0.001 min$^{-1}$ (●, $n = 8$). IRBP concentrations and removal rate constants are, in $\mu$M and min$^{-1}$, respectively: *1*, 0.020 ± 0.001 (○, $n = 6$); *2*, 0.036 ± 0.003 (▲, $n = 7$); *5*, 0.06 ± 0.01 (△, $n = 7$); *10*, 0.12 ± 0.02 (◆, $n = 8$); *20*, 0.29 ± 0.05 (◇, $n = 8$). *Error bars* represent standard deviations. The errors for the removal rate constants were obtained from the curve fits.

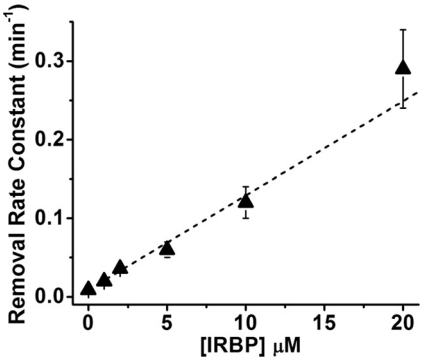


**Figure 3. Linear dependence of the rate constant of retinol removal on the extracellular IRBP concentration ($R = 0.99$).** The slope of the line is 0.012 ± 0.001 min$^{-1}$ $\mu$M$^{-1}$. Rate constant data are from the experiments shown in Fig. 2.

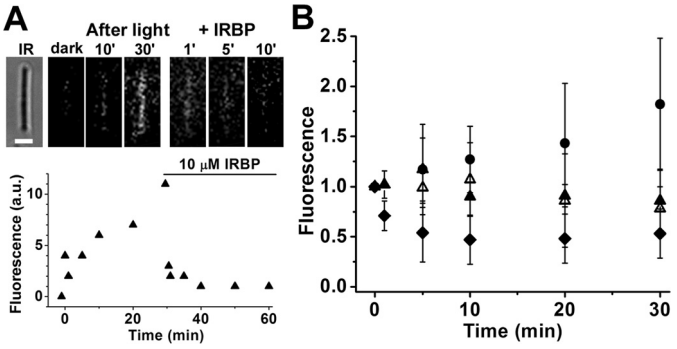


**Figure 4. Measurement of all-*trans*-retinal removal by different concentrations of IRBP in isolated metabolically compromised bROS from wild-type mice.** *A,* removal of all-*trans*-retinal released after bleaching by 10 $\mu$M IRBP. *IR,* infrared image of the cell; *bar,* 5 $\mu$m. Bleaching was carried out between $t = -1$ min and $t = 0$. IRBP was added 30 min after bleaching. Fluorescence images of the cell were acquired with 360 nm excitation and >420 nm emission. *B,* removal of all-*trans*-retinal by different concentrations of IRBP added at $t = 0$, 30 min after the bleaching of rhodopsin. Without addition of IRBP (●, $n = 10$), retinal fluorescence kept increasing. IRBP concentrations are in $\mu$M: 2 (▲, $n = 6$); 5 (△, $n = 7$); 10 (◆, $n = 7$). Retinal outer segment fluorescence intensities have been normalized over the value at $t = 0$. *Error bars* represent standard deviations.

dependence of the rate constant on IRBP concentration was linear, with a slope of 0.012 ± 0.001 min$^{-1}$ $\mu$M$^{-1}$ (Fig. 3).

### *Removal of all-trans-retinal by IRBP*

Broken-off rod outer segments (bROS), separated from the metabolic machinery of the inner segment, have no access to NADPH. Thus, bROS cannot reduce all-*trans*-retinal to -retinol (3, 6). Following rhodopsin bleaching in a wild-type mouse rod outer segment, there is a much smaller increase in outer segment fluorescence due to the released all-*trans*-retinal, which has a lower fluorescence quantum yield compared with retinol (3) (Fig. 4*A*). Addition of 10 $\mu$M IRBP at 30 min after bleaching resulted in the decline of outer segment fluorescence, reflecting the removal of all-*trans*-retinal by IRBP. This was a single experiment at one IRBP concentration. Fig. 4*B* shows the collected results from experiments with different concentrations of IRBP. As in Fig. 2*B*, to facilitate comparisons across cells and IRBP concentrations, the outer segment fluorescence was normalized to its value immediately after the addition of IRBP, and the data were then averaged. The continued increase in fluorescence in the absence of IRBP likely reflects the accumulation of all-*trans*-retinal as it continues to be released by photoactivated rhodopsin (32), but it does not leave the outer segment. Contrary to the situation with all-*trans*-retinol, fluorescence did not decline to zero after addition of IRBP, suggesting that, at least within the time scale of the experiment, the carrier cannot completely remove the all-*trans*-retinal present in the outer segment. The removal of all-*trans*-retinal could not be readily described as a first-order process, and so it was not possible to assign a removal rate constant for each IRBP concentration. Comparing the levels of fluorescence at 30 min after the addition of IRBP (corresponding to 60 min after bleaching), we did find that addition of 2 $\mu$M IRBP resulted in a significant decline in outer segment fluorescence compared with no addition of IRBP ($p = 0.004$, *t* test) and that 10 $\mu$M IRBP was more effective than 5 $\mu$M IRBP ($p = 0.04$, *t* test). No significant difference, however, was detected between the effectiveness of 2 and 5 $\mu$M IRBP ($p = 0.32$, *t* test). Because of the fragility of mouse bROS and the low fluorescence signal of all-*trans*-retinal, it was not possible to characterize retinal removal by IRBP to the same extent as for all-*trans*-retinol.

The outer segments of metabolically intact rods from *Rdh8*$^{-/-}$ mice are deficient in Rdh8, the enzyme that catalyzes the reduction of all-*trans*-retinal to -retinol (3, 4). Thus, although they have access to the metabolic machinery of the inner segment, and to NADPH, they also cannot reduce all-*trans*-retinal to -retinol. Following rhodopsin bleaching in *Rdh8*$^{-/-}$ rods, outer segment fluorescence increases, reflecting the accumulation of released all-*trans*-retinal. Addition of 5 $\mu$M IRBP at 30 min after bleaching resulted in decline of outer segment fluorescence (Fig. 5), indicating removal of all-*trans*-retinal by IRBP. As with wild-type bROS, the removal of all-*trans*-

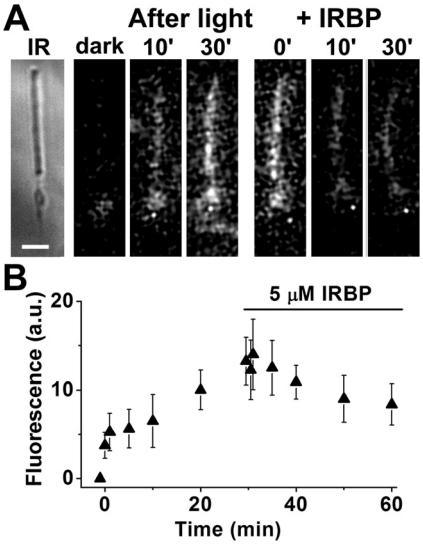


**Figure 5. Removal of all-*trans*-retinal by IRBP in isolated metabolically intact rod photoreceptors from *Rdh8*$^{-/-}$ mice, outer segments that lack Rdh8 cannot reduce the all-*trans*-retinal released after bleaching.** *A, IR,* infrared image of a metabolically intact rod photoreceptor cell isolated from an *Rdh8*$^{-/-}$ mouse; *bar,* 5 $\mu$m. Bleaching was carried out between $t = -1$ min and $t = 0$; 5 $\mu$M IRBP was added 30 min after bleaching. Fluorescence images were acquired with 360 nm excitation and >420 nm emission. *B,* rod outer segment fluorescence intensity after bleaching between $t = -1$ min and $t = 0$, and following the addition of 5 $\mu$M IRBP (▲, $n = 8$). *Error bars* represent standard deviations.

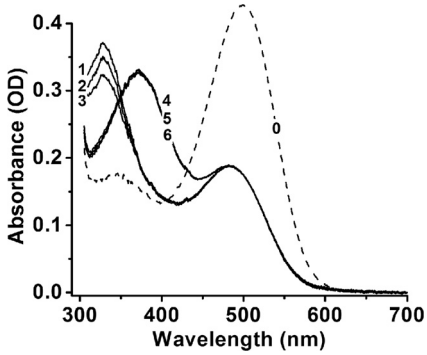


**Figure 6. Removal of all-*trans*-retinol by IRBP in purified bovine ROS membranes.** Rhodopsin (spectrum 0, concentration 10 $\mu$M) in purified ROS membranes was bleached for 5 min with >495 nm light in the presence of different concentrations of IRBP (0, 2, and 5 $\mu$M) and with or without NADPH (100 $\mu$M). After 30 min at 37 °C, in the presence of NADPH the released all-*trans*-retinal had been quantitatively converted to all-*trans*-retinol (*spectra 1–3*), whereas in the absence of NADPH it remained unconverted (*spectra 4–6*). In the absence of IRBP, both all-*trans*-retinol and all-*trans*-retinal remained in the membranes (*spectra 1* and *4*). 2 $\mu$M (*spectrum 2*) and 5 $\mu$M (*spectrum 3*) IRBP removed all-*trans*-retinol but had no effect on all-*trans*-retinal (*spectra 5* and *6*). To obtain the spectra, ROS membranes were solubilized in 1% Ammonyx LO at the end of incubation.

retinal in intact *Rdh8*$^{-/-}$ rods could not be readily described as a first-order process. Comparing the levels of outer segment fluorescence before and after the addition of IRBP, we found that 30 min of IRBP presence resulted in a significant decline (Fig. 5*B*; $p = 0.01$, paired $t$ test). We have not attempted to further characterize the interaction between IRBP and *Rdh8*$^{-/-}$ rods.

The results shown in Figs. 4 and 5 indicate that IRBP removes all-*trans*-retinal from outer segments. Upon comparison with the results in Fig. 2, it appears that IRBP is much less efficacious at removing all-*trans*-retinal than retinol. We have also exam-

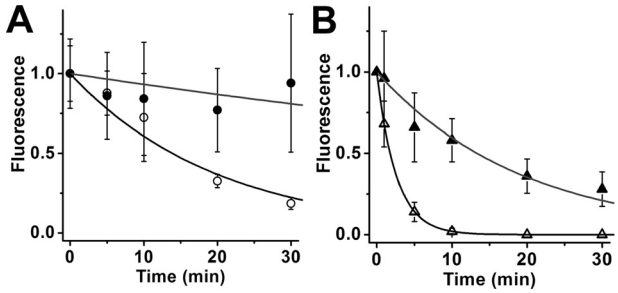


**Figure 7. Removal of exogenous all-*trans*-retinal and retinol from rod outer segments.** bROS from *Rpe65*$^{-/-}$ mice, containing negligible amounts of endogenous retinoids, were loaded with 50 $\mu$M retinal or retinol for 10 min, supplied with 1% BSA as carrier. Supply of exogenous retinoid was terminated at $t = 0$. Retinoid outer segment fluorescence intensities have been normalized over the value at $t = 0$. The lines are simple exponentials, $e^{-k \cdot t}$, decaying to 0 with unitary amplitude at $t = 0$ min, and have been drawn with rate constants $k$ determined from the experimental data points. *A,* removal of exogenous all-*trans*-retinal. In the absence of IRBP, retinal fluorescence declined with rate constant 0.007 ± 0.003 min$^{-1}$ (●, $n = 9$); in the presence of 5 $\mu$M IRBP, fluorescence decreased with rate constant 0.05 ± 0.01 min$^{-1}$ (○, $n = 4$). *B,* removal of exogenous all-*trans*-retinol. In the absence of IRBP, retinol fluorescence declined with rate constant 0.052 ± 0.005 min$^{-1}$ (▲, $n = 8$); in the presence of 5 $\mu$M IRBP, fluorescence decreased with rate constant 0.390 ± 0.002 min$^{-1}$ (△, $n = 5$). *Error bars* represent standard deviations. The *errors* for the removal rate constants were obtained from the curve fits.

ined the ability of IRBP to remove retinol and retinal from purified bovine ROS membranes (Fig. 6). Purified ROS membranes lack an NADPH source, and so any all-*trans*-retinal released after bleaching will not be reduced (spectra labeled *4,5,6* in Fig. 6). With addition of NADPH, however, all-*trans*-retinal is converted to all-*trans*-retinol (spectra labeled *1,2,3* in Fig. 6). 2 $\mu$M IRBP removed a fraction of 0.06 ± 0.01 (mean ± S.D.) of retinol, whereas 5 $\mu$M IRBP removed a fraction of 0.14 ± 0.03. IRBP was ineffective at removing all-*trans*-retinal, and for 2 $\mu$M IRBP, the difference was −0.01 ± 0.02 and for 5 $\mu$M IRBP was −0.03 ± 0.03.

We further examined this difference in efficacy in single bROS using exogenously added retinol and retinal. We loaded exogenous all-*trans*-retinal and retinol to bROS from *Rpe65*$^{-/-}$ mice, which contain negligible amounts of endogenous retinoids (33, 34); then, we measured their removal in the presence and absence of IRBP (5 $\mu$M concentration; Fig. 7). For these experiments, first-order kinetics provided a reasonable description of the removal of all-*trans*-retinal, presumably because of the high retinoid levels loaded (see "Discussion"). In the absence of IRBP, all-*trans*-retinal fluorescence declined very slowly, giving a removal rate constant of 0.007 ± 0.003 min$^{-1}$ (Fig. 7*A*). By contrast, the rate constant for the removal of all-*trans*-retinol in the absence of IRBP was ~7.4 times larger, 0.052 ± 0.005 min$^{-1}$ (Fig. 7*B*). The presence of 5 $\mu$M IRBP resulted in faster removal, with rate constants of 0.05 ± 0.01 min$^{-1}$ for retinal (Fig. 7*A*) and 0.390 ± 0.002 min$^{-1}$ for retinol (Fig. 7*B*); the rate constant for retinol removal was ~7.8 times larger than that for retinal.

### *Lower retinol and retinal levels after bleaching in the presence of IRBP*

In the retina of the living animal, rod outer segments are continuously bathed in the IRBP of the IPM. We therefore examined the effect of the continuous presence of physiological

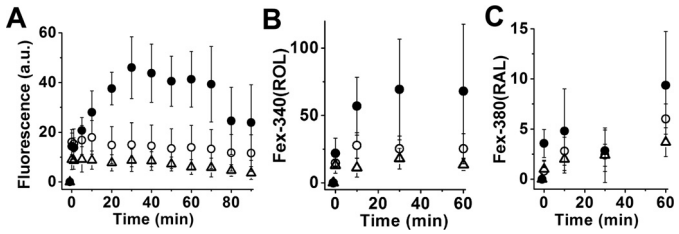


**Figure 8. Bleaching rod photoreceptors in the presence of IRBP results in strong reduction of outer segment fluorescence due to all-*trans*-retinol and all-*trans*-retinal.** Metabolically intact rod photoreceptors from wild-type mice were bleached in the absence and in the presence of different concentrations of IRBP. Bleaching took place between $t = -1$ and 0 min. *A,* outer segment fluorescence (excitation, 360 nm; emission, >420 nm) due to both all-*trans*-retinol and all-*trans*-retinal at different times after bleaching in the absence (●, $n = 8$) of IRBP and in the presence of 2 $\mu$M (○, $n = 10$) or 5 $\mu$M (△, $n = 13$) IRBP. *B* and *C*, outer segment fluorescence due to all-*trans*-retinol (*B*) and all-*trans*-retinal (*C*) at different times after bleaching in the absence (●, $n = 7$) of IRBP and in the presence of 2 $\mu$M (○, $n = 6$) or 5 $\mu$M (△, $n = 5$) IRBP. *B* and *C*, fluorescence signals Fex-340(ROL) and Fex-380(RAL) due, respectively, to all-*trans*-retinol and all-*trans*-retinal were measured simultaneously in the same cells. *Error bars* represent standard deviations.

concentrations of IRBP on the levels of retinal and retinol attained in rod outer segments after bleaching. Fig. 8*A* shows the effect of 2 and 5 $\mu$M IRBP on the levels of outer segment fluorescence (excitation, 360 nm; emission, >420 nm) attained after bleaching in metabolically intact wild-type rods. Fluorescence levels were significantly reduced in the presence of 2 $\mu$M IRBP ($p < 0.00001$ at 60 min after bleaching), and 5 $\mu$M IRBP reduced them significantly more than 2 $\mu$M ($p = 0.0036$ at 60 min after bleaching). The outer segment fluorescence signal excited by 360 nm is dominated by retinol but does include a contribution from retinal. The retinol and retinal signals can be separated by exciting outer segment fluorescence with 340 and 380 nm (10), and Fig. 8, *B* and *C,* shows the effect of IRBP on the individual retinoid levels. Retinol levels were significantly reduced by 2 $\mu$M IRBP, and 5 $\mu$M IRBP reduced them significantly more than 2 $\mu$M ($p = 0.042$ and $p = 0.036$ respectively, at 60 min after bleaching; Fig. 8*B*). Retinal levels were also reduced by IRBP, but the effect was statistically significant only for 5 $\mu$M IRBP ($p = 0.031$ at 60 min after bleaching; Fig. 8*C*).

### *IRBP prevents formation of lipofuscin precursors*

Addition of exogenous, or release of endogenous, all-*trans*-retinal in rod outer segments that cannot reduce it to retinol due to lack of access to sufficient amounts of NADPH has been shown to result in the formation of LFP fluorophores (35), likely to be bis-retinoids (36, 37). We first examined whether LFPs form after bleaching in the outer segments of metabolically intact rods that lack Rdh8. In the absence of the enzyme, the all-*trans*-retinal released by photoactivated rhodopsin is not reduced to retinol even though there is no lack of NADPH. Fig. 9*A* shows that in an intact *Rdh8*$^{-/-}$ mouse rod, there is an increase in the outer segment LFP fluorescence (excitation, 490 nm; emission, >515 nm) following rhodopsin bleaching. Results from *Rdh8*$^{-/-}$ rods (▲, $n = 12$; Fig. 9*B*) showed a significant increase in LFP fluorescence after bleaching ($p = 0.01$; linear regression with slope $0.027 \pm 0.007$). By contrast, in wild-type mouse rods (○, $n = 11$; Fig. 9*B*) there was no significant

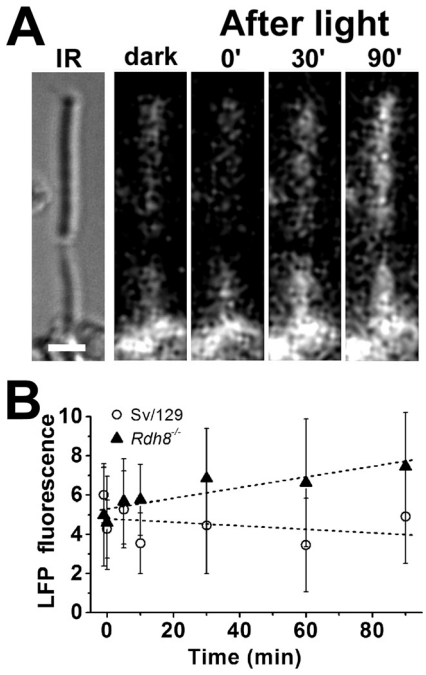


**Figure 9. Formation of LFP in metabolically rod photoreceptors of *Rdh8*$^{-/-}$ mice.** *A, IR,* infrared image of a rod photoreceptor cell isolated from an *Rdh8*$^{-/-}$ mouse; *bar,* 5 $\mu$m. Bleaching was carried out between $t = -1$ min and $t = 0$. Fluorescence images were acquired with 490 nm excitation and >515 nm emission. *B,* outer segment LFP fluorescence (excitation, 490 nm; emission, >515 nm) after bleaching in rod photoreceptors isolated from *Rdh8*$^{-/-}$ mice (▲, $n = 12$). Data from wild-type mice (○, $n = 11$) are re-plotted from Ref. 35 for comparison. *Error bars* represent standard deviations.

change in LFP fluorescence levels after rhodopsin bleaching ($p = 0.58$; linear regression with slope $-0.009 \pm 0.015$).

Because IRBP can remove all-*trans*-retinal, and all-*trans*-retinal can form LFPs, we then examined whether IRBP can prevent LFP formation after rhodopsin bleaching. Formation of LFPs after rhodopsin bleaching can be detected only in outer segments that cannot reduce all-*trans*-retinal, *i.e.* outer segments that lack either NADPH or Rdh8. We therefore measured LFP formation in bROS and in intact *Rdh8*$^{-/-}$ rods. Apart from wild-type rods, we also examined *Abca4*$^{-/-}$ rods, which accumulate high LFP levels due to the deletion of a transporter protein needed for efficient removal of retinal from outer segment disk membranes (36, 38). For an experiment, a dark-adapted rod was selected under infrared light, and the outer segment LFP fluorescence was measured. The rod was then bleached and kept in the dark, and LFP fluorescence was measured 60 min later (Fig. 10, *A* and *B*). The experiment was carried out with rods in the presence or absence of 5 $\mu$M IRBP.

For wild-type bROS, the presence of IRBP resulted in significantly less formation of LFP compared with control ($p = 0.0016$; Fig. 10*C*). The presence of IRBP also resulted in less LFP formation in *Abca4*$^{-/-}$ bROS (0.0048; Fig. 10*D*). Interestingly, IRBP had no detectable effect on the high LFP levels present in intact *Abca4*$^{-/-}$ rods ($p = 0.467$; Fig. 10*E*). Finally, the presence of IRBP did result in lower LFP levels in intact *Rdh8*$^{-/-}$ rods, but the difference was not statistically significant ($p = 0.05$; Fig. 10*F*).

Our findings are summarized in the schematic in Fig. 11, which illustrates the functional coupling of IRBP and RDH8

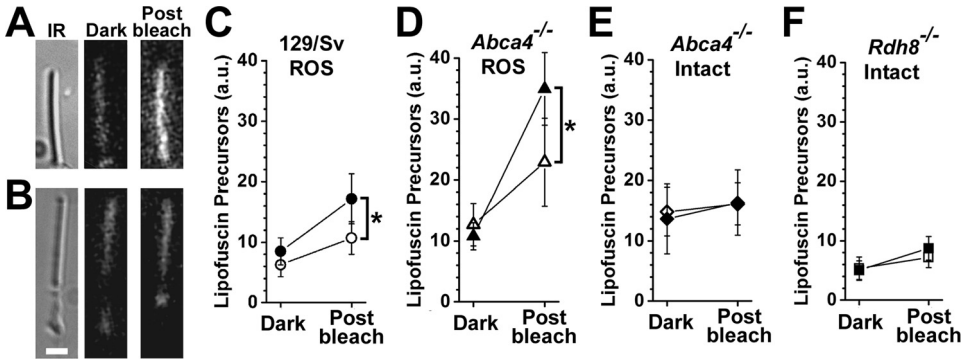


**Figure 10. IRBP prevents the formation of lipofuscin precursors but does not remove precursors already formed.** LFP levels were measured from rod outer segment fluorescence (excitation, 490 nm; emission, >515 nm) before bleaching (dark) and 60 min after bleaching (post-bleach). *A,* bROS from a 129/Sv mouse without added IRBP. *B,* metabolically intact rod photoreceptors from an *Abca4*$^{-/-}$ mouse without added IRBP. *Bar,* 5 $\mu$m. *C,* bROS from 129/Sv wild-type mice without added IRBP (●, $n = 6$) and in the presence of 5 $\mu$M IRBP (○, $n = 10$). *D,* bROS from *Abca4*$^{-/-}$ mice without added IRBP (▲, $n = 6$), and in the presence of 5 $\mu$M IRBP (△, $n = 8$). *E,* metabolically intact rod photoreceptors from *Abca4*$^{-/-}$ mice without added IRBP (♦, $n = 7$) and in the presence of 5 $\mu$M IRBP (◇, $n = 7$). *F,* metabolically intact rod photoreceptors from *Rdh8*$^{-/-}$ mice without added IRBP (■, $n = 11$) and in the presence of 5 $\mu$M IRBP (□, $n = 9$). *Asterisks* denote statistical significance. *Error bars* represent standard deviations.

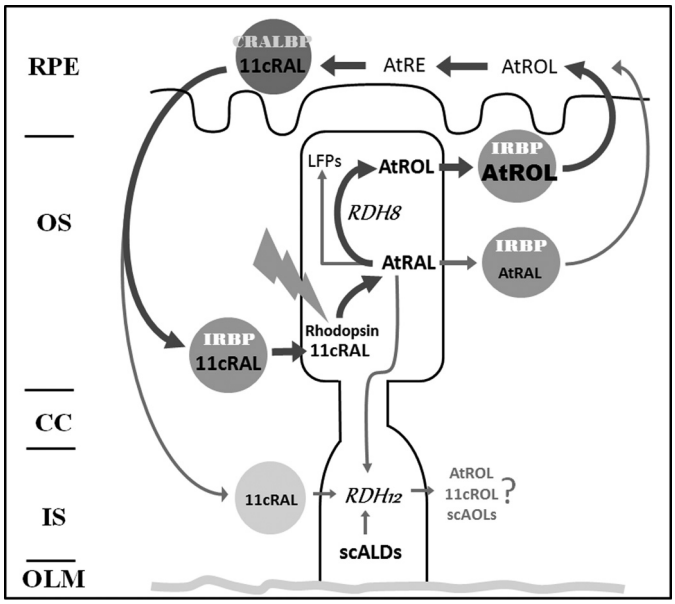


**Figure 11. Schematic of the functional coupling of IRBP and RDH8 that facilitates efficient removal of all-*trans*-retinol (*AtROL*) from photoreceptor outer segments following rhodopsin bleaching, which is necessary to prevent formation of LFPs.** Also shown are lesser pathways of all-*trans*-retinal (*AtRAL*) removal, involving direct interaction with IRBP, as well as leakage into the photoreceptor inner segment and reduction by RDH12, a broad specificity reductase for multiple short-chain aldehydes. *CRALBP,* cellular retinaldehyde-binding protein; *11cRAL,* 11-*cis*-retinal; *11cROL,* 11-*cis*-retinol; *scALDs,* short-chain aldehydes; *scAOLs,* short-chain alcohols; *RPE,* retinal pigment epithelium; *OS,* outer segment; *CC,* connecting cilium; *IS,* inner segment; *OLM,* outer limiting membrane.

that results in efficient removal of all-*trans*-retinal and all-*trans*-retinol from photoreceptor outer segments and in decreased formation of LFPs. Also shown are lesser pathways of all-*trans*-retinal removal, involving direct interaction with IRBP, as well as leakage into photoreceptor inner segments where it is reduced by RDH12 (3, 8). In addition to all-*trans*-retinal, the broad substrate specificity of RDH12 enables the reduction of 11-*cis*-retinal, as well as short chain aldehydes resulting from lipid peroxidation. Loss-of-function mutations in the gene encoding RDH12 are associated with Leber congenital amaurosis (39, 40).

## Discussion

Although the potential of IRBP to facilitate transport of retinoids between photoreceptors and RPE has been clear (20), the specific role of IRBP in visual cycle function has not been fully established. Consistent with the notion that IRBP might not be essential for the transport of retinoids between photoreceptors and RPE (22), this study shows that all-*trans*-retinol can leave mouse rod outer segments even in the absence of IRBP (Fig. 2), in agreement with previous results (31, 32). Early experiments also reported that the recovery kinetics of 11-*cis*-retinal levels following exposure to light are not significantly affected in mice that lack IRBP (23, 41), suggesting that IRBP may have only a marginal role in visual cycle activity. However, more recent studies demonstrated that mice that lack IRBP have slower rhodopsin regeneration kinetics and accumulate all-*trans*-retinal and retinol in the retina following light exposure (42). In addition, IRBP was shown to play a critical role in cone pigment regeneration (26, 42). One possibility that may account for the negative conclusions of the early experiments could be the use of mice harboring a variant of the Rpe65 protein that slows down the visual cycle (42).

This study shows that IRBP facilitates the removal of the all-*trans*-retinol generated after bleaching from mouse rods (Fig. 2). This is in agreement with previous findings in amphibian photoreceptors (30, 43, 44). One striking difference is that the rate constants for removal from mouse rods are much higher than those for frog rods (30); for example, the rate constant for removal by 1 $\mu$M IRBP is 0.020 $\pm$ 0.001 min$^{-1}$ for mouse compared with 0.007 $\pm$ 0.001 min$^{-1}$ for frog, whereas for 20 $\mu$M IRBP it is 0.29 $\pm$ 0.05 min$^{-1}$ compared with 0.061 $\pm$ 0.007 min$^{-1}$. One possible explanation is that with their diameter being about 5–6 times smaller than that of frog, mouse outer segments have a much larger surface-to-volume ratio, which would allow for faster removal of retinol. Another contributing factor may be that the IRBP used for both the mouse and frog experiments is of bovine origin, and it might be more effective for mammalian compared with amphibian rods. Another apparent difference is that in mouse rods the rate constant for retinol removal increases linearly with the IRBP concentration (Fig. 3), whereas in frog rods it appears to level off at

higher concentrations of IRBP (30). This leveling off in frog rods became evident at higher concentrations of IRBP, 50–100 $\mu$M; it was consistent with retinol removal involving the binding of IRBP to a plasma membrane receptor with an affinity of ~40 $\mu$M (30). In mouse rods, because of the high rates of retinol removal, it was not possible to accurately determine the removal rate constant for IRBP concentrations greater than 20 $\mu$M. The linear dependence of the removal rate constant on IRBP concentrations up to 20 $\mu$M is not inconsistent with the participation of a plasma membrane receptor that has an affinity for IRBP of ~40 $\mu$M. Our experiments, however, do not address the presence of an IRBP partner on the outer segment plasma membrane that may be playing a role in retinol removal (45). The removal of retinol is likely to be a complex multistep process, so its description with first-order rate constants is an approximation.

IRBP also facilitates the removal of all-*trans*-retinal from rod outer segments, and the removal is enhanced by increased concentrations of IRBP (Fig. 4). In contrast to retinol, not all of the all-*trans*-retinal generated by light in either bROS (Fig. 4) or in intact *Rdh8*$^{-/-}$ rod outer segments (Fig. 5) can be removed by IRBP, at least within the time scale of the experiments. Several considerations affect a straightforward interpretation of the results of Figs. 3 and 4. One, the fragility of the bROS limits the time scale of the experiments; two, the weak fluorescence of all-*trans*-retinal limits the signal-to-noise ratio of the measurements; three, it is possible that endogenously generated all-*trans*-retinal has specialized/non-specialized interactions with outer segment components that hinder its removal. The experiments of Fig. 7 addressed these concerns using *Rpe65*$^{-/-}$ mouse bROS, which contain negligible amounts of endogenous retinoids (33, 34), and loading them with high concentrations of exogenous all-*trans*-retinal and retinol. This also dramatically improved the signal-to-noise ratio of the all-*trans* fluorescence measurements and allowed quantification of the kinetics of retinal removal. Retinal left the bROS ~7.4 times more slowly than retinol in the absence of lipophilic carriers, and ~7.8 times more slowly than retinol in the presence of 5 $\mu$M IRBP. IRBP has comparable binding strengths for all-*trans*-retinal (0.195 $\mu$M) and all-*trans*-retinol (0.1–0.2 $\mu$M) (19), so it is unlikely that they are the explanation for the more efficacious removal of retinol. This is also consistent with the much slower removal of all-*trans*-retinal found in the absence of IRBP. Thus, the slower removal of all-*trans*-retinal appears to be due to its interaction with rod outer segment components, with an obvious possibility being reversible binding to phosphatidylethanolamine, which is present in high concentrations (46). Michael addition reactions with protein amino acid side chains, such as lysine's, is another possibility. The effect of such interactions would be even more pronounced at the lower concentrations of all-*trans*-retinal generated via release from photoactivated rhodopsin (Figs. 3 and 4). In contrast, all-*trans*-retinol, does not appear to interact strongly with outer segment components (47), allowing for its faster removal. This interpretation is further supported by the biochemical experiments of Fig. 6, showing that IRBP can remove the all-*trans*-retinol generated after the photoactivation of rhodopsin, but it is ineffective at removing all-*trans*-retinal. The difference in removal rates indicates that the reduction of all-*trans*-retinal to all-*trans*-retinol facilitates the faster clearance of the photoisomerized rhodopsin chromophore and its recycling. The reduction of all-*trans*-retinal to -retinol is dramatically impaired in mouse rod photoreceptors that lack both Rdh8 and Rdh12 (3, 48). Determination of retinoid levels in the eyes of these mice (48) shows delayed clearance of all-*trans*-retinal, consistent with a role for the reduction reaction in the facilitation of the removal.

The concentration of IRBP in the IPM varies significantly across species, at least from 2 to 13 $\mu$M. In rabbit and rat IPM, it was reported to be 2 and 3 $\mu$M, respectively (49). The results of Fig. 8 show that concentrations of IRBP in the physiological range, 2 and 5 $\mu$M, greatly reduce the levels of both all-*trans*-retinol and all-*trans*-retinal attained in rod outer segments after bleaching. Consistent with this effect, mice that lack IRBP have higher levels of all-*trans*-retinal and all-*trans*-retinol in the retina after light exposure compared with wild-type controls (42).

Accumulation of all-*trans*-retinal due to metabolic limitations has been shown to result in excess formation of LFPs in rod photoreceptor outer segments (10). All-*trans*-retinal also accumulates in *Rdh8*$^{-/-}$ rod outer segments, which lack the enzyme needed for the reduction of retinal to retinol (3, 48, 50). Fig. 9 shows that in *Rdh8*$^{-/-}$ rod outer segments, there is also increased LFP formation following light exposure, consistent with the increased accumulation of A2E in *Rdh8*$^{-/-}$ RPE (50, 51). Thus, accumulation of all-*trans*-retinal, regardless of cause, results in increased LFP formation.

IRBP can partially prevent the excess formation of LFPs that originate from all-*trans*-retinal accumulation in wild-type and *Abca4*$^{-/-}$ metabolically compromised rod outer segments (Fig. 10). Because IRBP has no effect on the levels of already formed LFPs (Fig. 10*C*), its effect is likely to be due to its ability to remove all-*trans*-retinal. We have not carried out any experiments to directly test a protective role for IRBP, but such a role is consistent with its protective effect against all-*trans*-retinal cytotoxicity (52), as well as with the increased accumulation of *bis*-retinoids in the RPE of IRBP-deficient mice (42).

In intact rods with a functioning Rdh8 enzyme, even in the absence of IRBP, it has not been possible to resolve any LFP formation from all-*trans*-retinal released by photoactivated rhodopsin (Fig. 10*C*) (10, 35). In the intact retina, rods will be in the presence of IRBP, which strongly promotes the clearance of all-*trans*-retinal (Fig. 8). This makes it unlikely that LFPs originate from free-dwelling all-*trans*-retinal, and it is consistent with the suggestion that they form from all-*trans*-retinal trapped in the form of a Schiff base with phosphatidylethanolamine (10). Another possibility would be that a small amount of chromophore remains trapped in aggregated opsin within which the Schiff base is retained.

In summary, we have examined the removal of all-*trans*-retinol and all-*trans*-retinal by IRBP from mouse rod outer segments. IRBP is much more efficacious in removing all-*trans*-retinol than all-*trans*-retinal, indicating an important role of the reduction reaction in the clearance of chromophore. The

extracellular presence of IRBP strongly suppresses the levels of both all-*trans*-retinol and all-*trans*-retinal following bleaching and limits the formation of LFPs from accumulated all-*trans*-retinal. The ability of IRBP to facilitate the clearance of all-*trans*-retinal from photoreceptor outer segments is strong evidence of an important role for IRBP in protecting against the cytotoxic effects of retinoids in the outer retina.

## Experimental procedures

### *Animals*

Wild-type (Sv/129) mice were from Harlan Laboratories (Indianapolis, IN). Animals were 2–5 months old, kept in cyclic light with a 12-h light cycle (06:00–18:00). All animal procedures were carried out in accordance with protocols approved by the Institutional Animal Care and Use Committees of the Medical University of South Carolina and of the University of Michigan, and with the recommendations of the Panel on Euthanasia of the American Veterinary Medical Association. For experiments, animals were dark-adapted overnight and sacrificed under dim-red light, and the retinas were excised under either dim-red or infrared light in mammalian physiological solution (in mM: 130 NaCl, 5 KCl, 0.5 $MgCl_2$, 2 $CaCl_2$, 25 hemisodium-HEPES, 5 glucose, pH 7.40). Isolated rod photoreceptor cells were obtained as described (31).

### *Materials*

Native IRBP was extracted from the soluble IPM fraction of bovine retinas and purified by a combination of concanavalin-A affinity, ion-exchange, and S-300 size-exclusion chromatography (53, 54). The concentration of the purified IRBP was determined by absorbance spectroscopy and amino acid analysis. Purified IRBP was shipped to Charleston on dry ice; before experiments, it was dialyzed with physiological solution containing 1 mM DTT (to prevent IRBP aggregation) using Amicon Ultra 0.5-ml centrifugal filters with 50-kDa cutoff (EMD Millipore, Billerica, MA). The final concentration of IRBP was estimated with absorption spectroscopy, using an extinction coefficient of $0.116 \times 10^6$ $M^{-1}$ $cm^{-1}$ at 280 nm (55). For an experiment, the solution containing IRBP was prepared to twice the desired final concentration; a volume of the IRBP solution was then added to an equal volume of the solution containing the photoreceptors. The final concentration of DTT, 0.5 mM, resulted in a slight increase in outer segment fluorescence, but control experiments showed that it did not affect the kinetics of retinol and retinal generation and removal. Other control experiments showed that freezing and thawing of IRBP did not affect its efficacy. All other reagents were from Sigma.

### *Fluorescence imaging*

Fluorescence measurements were carried out at 37 °C on the stage of an inverted Zeiss Axiovert 100 microscope (Carl Zeiss, Thornwood, NY) with a 40× oil immersion objective lens (NA = 1.3) (31). For measuring the overall rod outer segment retinol and retinal fluorescence signal, fluorescence was excited with a broadband (40-nm bandwidth) 360-nm filter, and the emission was collected through a long-pass 420-nm filter (emission, >420 nm). The particular excitation was selected to allow for comparison with extensive previously published data from mice (31, 32) as well as frogs (30). Previous work has established that in metabolically intact rods from wild-type and $Abca4^{-/-}$ mice, this fluorescence signal is mostly due to retinol; in metabolically intact rods from $Rdh8^{-/-}$ mice and in metabolically compromised bROS, it is mostly due to retinal (3, 6). Biochemical measurements of all-*trans*-retinol in excised retinas are in good agreement with single-cell fluorescence measurements (31, 32). For metabolically intact rods with adequate metabolic substrate, the contributions of retinal and retinol to outer segment fluorescence can be separated by exciting their fluorescence with narrow bandpass (10-nm bandwidth) filters centered at 340 and 380 nm (10). The contribution of retinol is referred to as Fex-340(ROL) and that of retinal as Fex-380(RAL). Experiments using excitation with both 340 and 380 nm have fewer time points, as we tried to minimize measuring light exposure to avoid retinoid photobleaching. LFP fluorescence was measured with 490 nm excitation and emission >515 nm (35). For measurements with endogenous fluorophores, fluorescence images were initially recorded for the dark-adapted cell; the cell was subsequently bleached with >530 nm of light for 1 min, and fluorescence images were recorded at different times after bleaching. For measurements with exogenously supplied retinal and retinol to $Rpe65^{-/-}$ bROS, bovine serum albumin was used as a lipophilic carrier (at 1% concentration) (3). In these loading experiments, the bROS is exposed to a bath solution containing the retinoid-carrying BSA for 10 min, and not all of the retinoid on the BSA present in the bathing solution is transferred to the bROS. Image acquisition and analysis were carried out using Slidebook (Intelligent Imaging Innovations, Denver, CO).

### *Experiments with bovine ROS membranes*

ROS were prepared from frozen bovine retinas as described previously (32). Purified membranes were suspended in physiological solution at a rhodopsin concentration of 20 $\mu$M. An aliquot was removed and diluted to 10 $\mu$M to serve as the unbleached reference (*spectrum 0* in Fig. 6). The rest was bleached at room temperature for 5 min, and divided into six samples. All subsequent manipulations were carried out under dim red light. NADPH (final concentration 100 $\mu$M) was added to three of the samples as well as IRBP (final concentrations 0, 2, and 5 $\mu$M). The final rhodopsin concentration was 10 $\mu$M. After incubating at 37 °C for 30 min, samples were centrifuged in an Eppendorf refrigerated 5415R centrifuge for 10 min at 16,100 × *g*. After two washes with physiological solution to remove NADPH, the resulting pellets were solubilized in 1% *N*,*N*-dimethyldodecylamine *N*-oxide (Ammonyx LO) and spun to remove any unsolubilized material, and the supernatants were scanned on a Cary 300 spectrophotometer. The experiment was repeated three times.

### *Statistical analysis*

Statistical significance was tested with *t* test and linear regression. In the figures, statistically significant differences are indicated with an asterisk.

*Author contributions*—C. C., L. A., and P. G. carried out most of the experiments and analyzed the data; F. G.-F., D. A. T., and Y. K. designed the experiments, analyzed the data, and wrote the paper.

*Acknowledgments—We thank Kecia Feathers, Lin Jia, Nirosha Perera, and Austra Liepa for expert technical assistance; John M. Nickerson for Irbp-deficient (Rbp3$^{-/-}$) mice; Krzysztof Palczewski for Rdh8-deficient mice; T. Michael Redmond for Rpe65-deficient mice; and Gabriel H. Travis for Abca4-deficient mice. An unrestricted grant to the Dept. of Ophthalmology at Medical University of South Carolina was provided by Research to Prevent Blindness (New York), and an unrestricted grant to the Dept. of Ophthalmology and Visual Sciences at the University of Michigan Medical School was provided by Research to Prevent Blindness (New York). This work utilized the Vision Research Core funded by National Institutes of Health Grant P30 EY007003 from the NEI. This work was conducted in a facility constructed with support from National Institutes of Health Grant C06 RR015455 from the Extramural Research Facilities Program of the National Center for Research Resources.*

## References


1. Ebrey, T., and Koutalos, Y. (2001) Vertebrate photoreceptors. *Prog. Retin. Eye Res.* **20,** 49–94
2. Wald, G. (1968) Molecular basis of visual excitation. *Science* **162,** 230–239
3. Chen, C., Thompson, D. A., and Koutalos, Y. (2012) Reduction of all-*trans*-retinal in vertebrate rod photoreceptors requires the combined action of RDH8 and RDH12. *J. Biol. Chem.* **287,** 24662–24670
4. Maeda, A., Maeda, T., Imanishi, Y., Kuksa, V., Alekseev, A., Bronson, J. D., Zhang, H., Zhu, L., Sun, W., Saperstein, D. A., Rieke, F., Baehr, W., and Palczewski, K. (2005) Role of photoreceptor-specific retinol dehydrogenase in the retinoid cycle *in vivo*. *J. Biol. Chem.* **280,** 18822–18832
5. Rattner, A., Smallwood, P. M., and Nathans, J. (2000) Identification and characterization of all-*trans*-retinol dehydrogenase from photoreceptor outer segments, the visual cycle enzyme that reduces all-*trans*-retinal to all-*trans*-retinol. *J. Biol. Chem.* **275,** 11034–11043
6. Adler, L., 4th, Chen, C., and Koutalos, Y. (2014) Mitochondria contribute to NADPH generation in mouse rod photoreceptors. *J. Biol. Chem.* **289,** 1519–1528
7. Futterman, S., Hendrickson, A., Bishop, P. E., Rollins, M. H., and Vacano, E. (1970) Metabolism of glucose and reduction of retinaldehyde in retinal photoreceptors. *J. Neurochem.* **17,** 149–156
8. Chrispell, J. D., Feathers, K. L., Kane, M. A., Kim, C. Y., Brooks, M., Khanna, R., Kurth, I., Hübner, C. A., Gal, A., Mears, A. J., Swaroop, A., Napoli, J. L., Sparrow, J. R., and Thompson, D. A. (2009) Rdh12 activity and effects on retinoid processing in the murine retina. *J. Biol. Chem.* **284,** 21468–21477
9. Parish, C. A., Hashimoto, M., Nakanishi, K., Dillon, J., and Sparrow, J. (1998) Isolation and one-step preparation of A2E and iso-A2E, fluorophores from human retinal pigment epithelium. *Proc. Natl. Acad. Sci. U.S.A.* **95,** 14609–14613
10. Adler, L., 4th, Chen, C., and Koutalos, Y. (2017) All-trans retinal levels and formation of lipofuscin precursors after bleaching in rod photoreceptors from wild type and Abca4−/− mice. *Exp. Eye Res.* **155,** 121–127
11. Sparrow, J. R., Gregory-Roberts, E., Yamamoto, K., Blonska, A., Ghosh, S. K., Ueda, K., and Zhou, J. (2012) The bisretinoids of retinal pigment epithelium. *Prog. Retin. Eye Res.* **31,** 121–135
12. Lamb, T. D., and Pugh, E. N., Jr. (2004) Dark adaptation and the retinoid cycle of vision. *Prog. Retin. Eye Res.* **23,** 307–380
13. Saari, J. C. (2000) Biochemistry of visual pigment regeneration: the Friedenwald lecture. *Invest. Ophthalmol. Vis. Sci.* **41,** 337–348
14. Tang, P. H., Kono, M., Koutalos, Y., Ablonczy, Z., and Crouch, R. K. (2013) New insights into retinoid metabolism and cycling within the retina. *Prog. Retin. Eye Res.* **32,** 48–63
15. Szuts, E. Z., and Harosi, F. I. (1991) Solubility of retinoids in water. *Arch. Biochem. Biophys.* **287,** 297–304
16. Moise, A. R., Noy, N., Palczewski, K., and Blaner, W. S. (2007) Delivery of retinoid-based therapies to target tissues. *Biochemistry* **46,** 4449–4458
17. Gonzalez-Fernandez, F. (2003) Interphotoreceptor retinoid–binding protein–an old gene for new eyes. *Vision Res.* **43,** 3021–3036
18. Gonzalez-Fernandez, F., and Ghosh, D. (2008) Focus on molecules: interphotoreceptor retinoid-binding protein (IRBP). *Exp. Eye Res.* **86,** 169–170
19. Chen, Y., and Noy, N. (1994) Retinoid specificity of interphotoreceptor retinoid-binding protein. *Biochemistry* **33,** 10658–10665
20. Okajima, T. I., Pepperberg, D. R., Ripps, H., Wiggert, B., and Chader, G. J. (1989) Interphotoreceptor retinoid-binding protein: role in delivery of retinol to the pigment epithelium. *Exp. Eye Res.* **49,** 629–644
21. Okajima, T. I., Pepperberg, D. R., Ripps, H., Wiggert, B., and Chader, G. J. (1990) Interphotoreceptor retinoid-binding protein promotes rhodopsin regeneration in toad photoreceptors. *Proc. Natl. Acad. Sci. U.S.A.* **87,** 6907–6911
22. Ho, M. T., Massey, J. B., Pownall, H. J., Anderson, R. E., and Hollyfield, J. G. (1989) Mechanism of vitamin A movement between rod outer segments, interphotoreceptor retinoid-binding protein, and liposomes. *J. Biol. Chem.* **264,** 928–935
23. Palczewski, K., Van Hooser, J. P., Garwin, G. G., Chen, J., Liou, G. I., and Saari, J. C. (1999) Kinetics of visual pigment regeneration in excised mouse eyes and in mice with a targeted disruption of the gene encoding interphotoreceptor retinoid-binding protein or arrestin. *Biochemistry* **38,** 12012–12019
24. Gonzalez-Fernandez, F., Betts-Obregon, B., Yust, B., Mimun, J., Sung, D., Sardar, D., and Tsin, A. T. (2015) Interphotoreceptor retinoid-binding protein protects retinoids from photodegradation. *Photochem. Photobiol.* **91,** 371–378
25. Gonzalez-Fernandez, F., Sung, D., Haswell, K. M., Tsin, A., and Ghosh, D. (2014) Thiol-dependent antioxidant activity of interphotoreceptor retinoid-binding protein. *Exp. Eye Res.* **120,** 167–174
26. Parker, R., Wang, J. S., Kefalov, V. J., and Crouch, R. K. (2011) Interphotoreceptor retinoid-binding protein as the physiologically relevant carrier of 11-cis-retinol in the cone visual cycle. *J. Neurosci.* **31,** 4714–4719
27. den Hollander, A. I., McGee, T. L., Ziviello, C., Banfi, S., Dryja, T. P., Gonzalez-Fernandez, F., Ghosh, D., and Berson, E. L. (2009) A homozygous missense mutation in the IRBP gene (RBP3) associated with autosomal recessive retinitis pigmentosa. *Invest. Ophthalmol. Vis. Sci.* **50,** 1864–1872
28. Liou, G. I., Fei, Y., Peachey, N. S., Matragoon, S., Wei, S., Blaner, W. S., Wang, Y., Liu, C., Gottesman, M. E., and Ripps, H. (1998) Early onset photoreceptor abnormalities induced by targeted disruption of the interphotoreceptor retinoid-binding protein gene. *J. Neurosci.* **18,** 4511–4520
29. Adler, L., 4th, Boyer, N. P., Chen, C., and Koutalos, Y. (2015) Kinetics of rhodopsin's chromophore monitored in a single photoreceptor. *Methods Mol. Biol.* **1271,** 327–343
30. Wu, Q., Blakeley, L. R., Cornwall, M. C., Crouch, R. K., Wiggert, B. N., and Koutalos, Y. (2007) Interphotoreceptor retinoid-binding protein is the physiologically relevant carrier that removes retinol from rod photoreceptor outer segments. *Biochemistry* **46,** 8669–8679
31. Chen, C., Blakeley, L. R., and Koutalos, Y. (2009) Formation of all-*trans*-retinol after visual pigment bleaching in mouse photoreceptors. *Invest. Ophthalmol. Vis. Sci.* **50,** 3589–3595
32. Blakeley, L. R., Chen, C., Chen, C. K., Chen, J., Crouch, R. K., Travis, G. H., and Koutalos, Y. (2011) Rod outer segment retinol formation is independent of Abca4, arrestin, rhodopsin kinase, and rhodopsin palmitylation. *Invest. Ophthalmol. Vis. Sci.* **52,** 3483–3491
33. Chen, C., Tsina, E., Cornwall, M. C., Crouch, R. K., Vijayaraghavan, S., and Koutalos, Y. (2005) Reduction of all-*trans*-retinal to all-*trans*-retinol in the outer segments of frog and mouse rod photoreceptors. *Biophys. J.* **88,** 2278–2287
34. Redmond, T. M., Yu, S., Lee, E., Bok, D., Hamasaki, D., Chen, N., Goletz, P., Ma, J. X., Crouch, R. K., and Pfeifer, K. (1998) Rpe65 is necessary for production of 11-cis-vitamin A in the retinal visual cycle. *Nat. Genet.* **20,** 344–351

35. Boyer, N. P., Higbee, D., Currin, M. B., Blakeley, L. R., Chen, C., Ablonczy, Z., Crouch, R. K., and Koutalos, Y. (2012) Lipofuscin and *N*-retinylidene-*N*-retinylethanolamine (A2E) accumulate in retinal pigment epithelium in absence of light exposure: their origin is 11-*cis*-retinal. *J. Biol. Chem.* **287,** 22276–22286
36. Quazi, F., and Molday, R. S. (2014) ATP-binding cassette transporter ABCA4 and chemical isomerization protect photoreceptor cells from the toxic accumulation of excess 11-cis-retinal. *Proc. Natl. Acad. Sci. U.S.A.* **111,** 5024–5029
37. Ueda, K., Zhao, J., Kim, H. J., and Sparrow, J. R. (2016) Photodegradation of retinal bisretinoids in mouse models and implications for macular degeneration. *Proc. Natl. Acad. Sci. U.S.A.* **113,** 6904–6909
38. Weng, J., Mata, N. L., Azarian, S. M., Tzekov, R. T., Birch, D. G., and Travis, G. H. (1999) Insights into the function of Rim protein in photoreceptors and etiology of Stargardt's disease from the phenotype in abcr knockout mice. *Cell* **98,** 13–23
39. Janecke, A. R., Thompson, D. A., Utermann, G., Becker, C., Hübner, C. A., Schmid, E., McHenry, C. L., Nair, A. R., Rüschendorf, F., Heckenlively, J., Wissinger, B., Nürnberg, P., and Gal, A. (2004) Mutations in RDH12 encoding a photoreceptor cell retinol dehydrogenase cause childhood-onset severe retinal dystrophy. *Nat. Genet.* **36,** 850–854
40. Perrault, I., Hanein, S., Gerber, S., Barbet, F., Ducroq, D., Dollfus, H., Hamel, C., Dufier, J. L., Munnich, A., Kaplan, J., and Rozet, J. M. (2004) Retinal dehydrogenase 12 (RDH12) mutations in leber congenital amaurosis. *Am. J. Hum. Genet.* **75,** 639–646
41. Ripps, H., Peachey, N. S., Xu, X., Nozell, S. E., Smith, S. B., and Liou, G. I. (2000) The rhodopsin cycle is preserved in IRBP "knockout" mice despite abnormalities in retinal structure and function. *Vis. Neurosci.* **17,** 97–105
42. Jin, M., Li, S., Nusinowitz, S., Lloyd, M., Hu, J., Radu, R. A., Bok, D., and Travis, G. H. (2009) The role of interphotoreceptor retinoid-binding protein on the translocation of visual retinoids and function of cone photoreceptors. *J. Neurosci.* **29,** 1486–1495
43. Ala-Laurila, P., Kolesnikov, A. V., Crouch, R. K., Tsina, E., Shukolyukov, S. A., Govardovskii, V. I., Koutalos, Y., Wiggert, B., Estevez, M. E., and Cornwall, M. C. (2006) Visual cycle: dependence of retinol production and removal on photoproduct decay and cell morphology. *J. Gen. Physiol.* **128,** 153–169
44. Tsina, E., Chen, C., Koutalos, Y., Ala-Laurila, P., Tsacopoulos, M., Wiggert, B., Crouch, R. K., and Cornwall, M. C. (2004) Physiological and microfluorometric studies of reduction and clearance of retinal in bleached rod photoreceptors. *J. Gen. Physiol.* **124,** 429–443
45. Garlipp, M. A., and Gonzalez-Fernandez, F. (2013) Cone outer segment and Muller microvilli pericellular matrices provide binding domains for interphotoreceptor retinoid-binding protein (IRBP). *Exp. Eye Res.* **113,** 192–202
46. Fliesler, S. J., and Anderson, R. E. (1983) Chemistry and metabolism of lipids in the vertebrate retina. *Prog. Lipid Res.* **22,** 79–131
47. Wu, Q., Chen, C., and Koutalos, Y. (2006) All-trans retinol in rod photoreceptor outer segments moves unrestrictedly by passive diffusion. *Biophys. J.* **91,** 4678–4689
48. Maeda, A., Maeda, T., Sun, W., Zhang, H., Baehr, W., and Palczewski, K. (2007) Redundant and unique roles of retinol dehydrogenases in the mouse retina. *Proc. Natl. Acad. Sci. U.S.A.* **104,** 19565–19570
49. Adler, A. J., and Edwards, R. B. (2000) Human interphotoreceptor matrix contains serum albumin and retinol-binding protein. *Exp. Eye Res.* **70,** 227–234
50. Maeda, A., Maeda, T., Golczak, M., and Palczewski, K. (2008) Retinopathy in mice induced by disrupted all-*trans*-retinal clearance. *J. Biol. Chem.* **283,** 26684–26693
51. Maeda, A., Golczak, M., Maeda, T., and Palczewski, K. (2009) Limited roles of Rdh8, Rdh12, and Abca4 in all-*trans*-retinal clearance in mouse retina. *Invest. Ophthalmol. Vis. Sci.* **50,** 5435–5443
52. Lee, M., Li, S., Sato, K., and Jin, M. (2016) Interphotoreceptor retinoid-binding protein mitigates cellular oxidative stress and mitochondrial dysfunction induced by all-*trans*-retinal. *Invest. Ophthalmol. Vis. Sci.* **57,** 1553–1562
53. Liou, G. I., Fong, S. L., Beattie, W. G., Cook, R. G., Leone, J., Landers, R. A., Alvarez, R. A., Wang, C., Li, Y., and Bridges, C. D. (1986) Bovine interstitial retinol-binding protein (IRBP)–isolation and sequence analysis of cDNA clones, characterization and *in vitro* translation of mRNA. *Vision Res.* **26,** 1645–1653
54. Saari, J. C., Teller, D. C., Crabb, J. W., and Bredberg, L. (1985) Properties of an interphotoreceptor retinoid-binding protein from bovine retina. *J. Biol. Chem.* **260,** 195–201
55. Adler, A. J., and Evans, C. D. (1985) Some functional characteristics of purified bovine interphotoreceptor retinol-binding protein. *Invest. Ophthalmol. Vis. Sci.* **26,** 273–282